Rare Metal Materials and Engineering
Volume 50, Issue 10, October 2021
Available online at www.rmme.ac.cn

Science Press

Cite this article as: Su Hui, Chu Zhibing, Xue Chun, et al. Tension-Compression Asymmetry and Microstructure of Extruded AZ31 Magnesium Alloy[J]. Rare Metal Materials and Engineering, 2021, 50(10): 3446-3453.

ARTICLE

Tension-Compression Asymmetry and Microstructure of Extruded AZ31 Magnesium Alloy

Su Hui[1], Chu Zhibing[1,2], Xue Chun[1], Li Yugui[1], Ma Lifeng[1]

[1] Engineering Research Center Heavy Machinery Ministry of Education, Taiyuan University of Science and Technology, Taiyuan 030024, China; [2] School of Mechanics and Architectural Engineering, Jinan University, Guangzhou 510632, China

Abstract: The mechanical behavior and texture evolution of extruded AZ31 magnesium alloy during the axial tension-compression process at room temperature were simulated by a modified viscoplastic self-consistent model considering slip and twin plastic deformation mechanisms. On the basis of EBSD experiment and simulation, the mechanism of tension-compression asymmetry caused by different deformation mechanisms and the texture evolution in the process of plastic deformation were analyzed. Results show that basal slip is the main deformation mode in the early stage of axial tension deformation, but the orientation factor of basal slip is low and has a hard orientation, resulting in higher yield stress. With the increase in strain, prismatic slip becomes the main deformation mechanism, and the strain hardening rate is low, so the stress-strain curve is smooth. In the early stage of axial compression, tension twinning has a high activity due to its low critical shear stress, leading to lower yield stress. As the relative activity decreases rapidly with the tension twinning, the hardening rate increases at the same time. In the later stage, with the activation of compression twinning, its relative activity increases rapidly; the accumulated stress during plastic deformation can be released, and the hardening rate decreases. In addition, the less twin volume fraction in the ED direction was explained by the color and the twin trace of typical grain.

Key words: viscoplastic self-consistent model; tension-compression asymmetry; texture evolution; plastic deformation mechanism

Magnesium alloy has high specific strength, high specific stiffness, good damping performance, and good thermal conductivity, thus being an important choice for material application in the fields of automobile, communication, and military industry[1-3]. AZ31 alloy is one of the most widely applied materials among magnesium alloys. The texture evolution of magnesium alloy has a significant effect on its properties[4-7]. For example, magnesium alloy will form a strong basal texture after rolling, and will form a strong basal fiber texture after extruding, thus showing obvious tension-compression asymmetry. Once the texture is formed in the magnesium alloy, it easily shows relatively obvious anisotropy, which greatly affects the subsequent deformation ability and hinders its application and development. Therefore, the micromechanism and texture evolution of the tension-compression asymmetry during plastic deformation of magnesium alloys should be studied to predict the properties of magnesium alloys[8].

At present, the most commonly used technical methods for analyzing material texture are X-ray diffraction (XRD) and electron back scattering diffraction (EBSD). However, the shortcomings of these two experimental methods are high cost of testing, difficulty of sample preparation, and long experimental period. Based on the common optical reflection method, Gaskey et al[9] has realized the grain orientation characterization of metal Ni and semiconductor silicon wafers using the directional reflection microscope (DRM). However, the disadvantages of this experimental method are inability to study quantitatively the effects of slip and twinning on the texture evolution. With the rapid development of computational materials[10], researchers have focused on establishing a computational model of crystal plasticity on the basis of theory of crystal plasticity and the influence of deformation mechanisms[11], such as slip and twinning on the texture evolution of metals in the plastic deformation process from the microscopic perspective. The viscoplastic self-consistent

Received date: October 13, 2020
Corresponding author: Chu Zhibing, Ph. D., Professor, College of Materials Science and Engineering, Taiyuan University of Technology, Taiyuan 030024, P. R. China, E-mail: piegen@163.com

(VPSC) model proposed by Lebensohn and Tomé[12] is the most representative model. The stress and strain coordination at the grain boundary is satisfied, and the large deformation behavior of polycrystalline materials can be simulated and predicted. The VPSC model has been successfully used to simulate the macroscopic mechanical response and micro-texture evolution of magnesium alloys[13,14].

Although VPSC models have been applied to AZ31[15] repeatedly, a comprehensive work that employs VPSC models to simulate a vast collection of mechanical and micro-structural measurements remains lacking. In this work, the deformation process of the extruded AZ31 magnesium alloy was studied through axial tensile and compression tests, XRD, and EBSD experiments at room temperature. The experiment was numerically simulated by a modified VPSC model. From the perspective of the micro-deformation mechanism, the mechanism of tensile and compression asymmetry and the evolution law of microstructure of extruded AZ31 magnesium alloy were investigated. This study is a useful guideline for future researchers regarding the use of texture to strengthen or improve mechanical properties and formation performance.

1 Viscoplastic Self-Consistent Model

In physics, when the plastic behavior of two adjacent single crystals satisfying the conditions of geometric coordination and stress balance is determined, the plastic behavior of polycrystals can be described depending on the transformation from micro-physical quantity to macro-physical quantity. The VPSC model considers the interaction between grains in polycrystals and assumes that the grains are ellipsoid. It is included and buried deep in a homogeneous equivalent medium, and the model adopts the following rate-dependent continuous constitutive model equation[12]:

$$\varepsilon_{ij}(\bar{x})=\sum_s m_{ij}^s\gamma^s(\bar{x})=\gamma_0\sum_s m_{ij}^s\left\{\frac{m_{kl}^s\sigma_{kl}(\bar{x})}{\tau^s}\right\}^n=M_{ijkl}\sigma_{kl}(\bar{x}) \quad (1)$$

where τ^s denotes the critical shear stress; $m_{ij}^s=\frac{1}{2}(n_i^s b_j^s+b_j^s n_i^s)$ is the Schmid factor of the slip/twin system (s); n^s and b^s represent the normal direction (ND) of the slip/twin plane and the slip/twin direction, respectively; $\varepsilon_{ij}(\bar{x})$ and $\sigma_{kl}(\bar{x})$ are the strain and stress partial tensors, respectively; γ^s stands for the local shear rate acting on the slip system (s); γ_0 represents the normalized coefficient; n is the rate sensitivity index; M_{ijkl} stands for the viscoplastic convention and can relate the macroscopic strain rate to the macroscopic deviatoric stress.

The critical shear stress τ^s is formed with the accumulation of shear amount in each grain. Therefore, the evolution rules can be described by the Voce hardening model:

$$\tau^s=\tau_0^s+(\tau_1^s+\theta_1^s\Gamma)\left[1-\exp\left(-\frac{\theta_0^s\Gamma}{\tau_1^s}\right)\right] \quad (2)$$

where $\Gamma=\sum_s\Delta\gamma^s$ is the cumulative shear of the grain, τ_0 denotes the initial critical stress, θ_0 stands for the initial hardening rate, θ_1 refers to the saturation hardening rate, and τ_0^s and τ_1^s are the initial and extrapolated critical shear stresses of mechanisms, respectively. Fig.1 depicts the specific definitions.

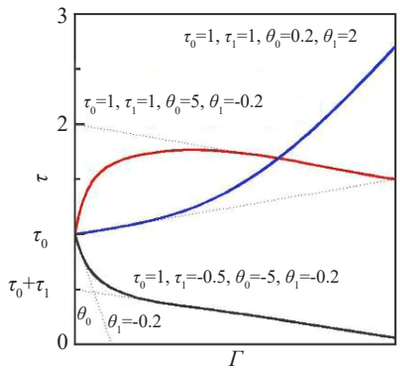

Fig.1 Physical meaning of hardening parameters for VPSC simulations

In this study, predominant twin reorientation (PTR)[16] was used to analyze the effect of twins on texture evolution during plastic deformation. For grain g, $\gamma^{t,g}$ is the shear strain caused by twin t, and the corresponding twin volume fraction is $V^{t,g}=\gamma^{t,g}/S^t$, where S^t is the intrinsic shear strain of twin system t.

The integral number of twins caused by all twin systems in all grains is called the cumulative twin integral number:

$$V^{acc,mode}=\sum_g\sum_t\gamma^{t,g}/S^t \quad (3)$$

Through superimposition of the twin fraction of each incremental step, the cumulative twin fraction is compared with the critical volume fraction caused by twins [17]. Thus, the critical volume fraction is defined as:

$$V^{th,mode}=A^{th1}+A^{th2}\frac{V^{eff,mode}}{V^{acc,mode}} \quad (4)$$

where $V^{eff,mode}$ is the effective twin crystal integral number, and A^{th1} and A^{th2} are material constants.

2 Numerical and Experimental Procedures

2.1 Experimental materials

The initial material selected was a commercial extruded AZ31 magnesium alloy bar with a diameter of 40 mm. Tension and compression experiments were conducted in the extrusion direction (ED), as shown in Fig. 2. The tensile sample had a dumbbell shape with a total length of 36 mm, a gauge length of 15 mm, and a cross-section size of 5 mm×1 mm. The compressed sample was a cuboid with dimensions of 8 mm×8 mm×12 mm and loading direction along the long axis. Tensile and compression tests were carried out at room temperature, and the strain rate was 10^{-3} s^{-1}.

Fig.3 shows the samples after axial tensile and compression fracture. Both samples are approximately fractured at 45° angle because when the sample is subjected to stress deformation, it has the maximum shear stress on the oblique section with an axial direction of 45°.

2.2 Numerical model

The extrusion direction of magnesium alloy is expressed by ED, and the transverse and normal directions perpendicular to the extrusion direction are expressed by TD and ND,

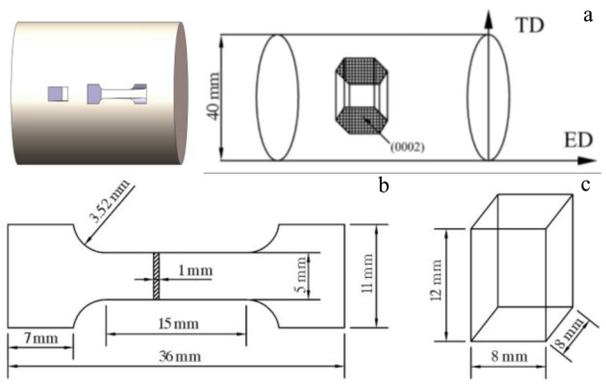

Fig.2 Schematic of samples (a), tension sample (b) and compression sample (c)

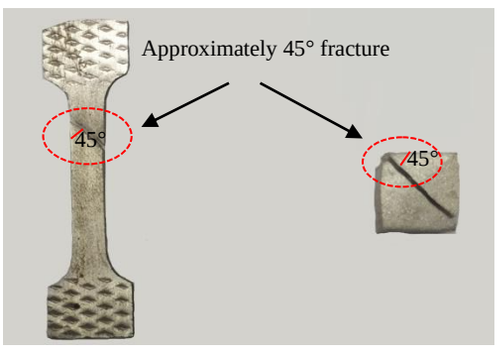

Fig.3 Tension and compression samples after fracture

respectively. The inverse pole diagram of the three faces of the magnesium alloy was measured by EBSD technology and combined into a three-dimensional microstructure, as shown in Fig.4a. Most of the initial samples have an equiaxed crystal structure, and the average grain size is 38 μm. In addition, some elongated grains can be found due to the grain stretching along the ED during extrusion. The corresponding inverse pole figure is shown in Fig. 4b. The original pole figure obtained by EBSD and XRD is shown in Fig.4c and 4d. Most of the *c*-axis of the grain is perpendicular to the ED, that is, the basal plane is parallel to the ED, resulting in a strong basal texture in the initial pole figure distribution of magnesium alloy. The texture component tends to be distributed homogeneously along the arc between [10$\bar{1}$0]//ED and [2$\bar{1}\bar{1}$0]//ED. The comparison of texture results shows that the macro-texture and micro-texture measured by XRD and EBSD have good consistency, which ensures the accuracy of the experimental results.

Considering the complexity of the deformation mechanism of magnesium alloy, obtaining all parameters through a single loading experiment is difficult. In this study, the optimal hardening parameters of different deformation mechanisms were determined by fitting the axial tensile and compressive stress-strain curves along the ED, as shown in Table 1. Results

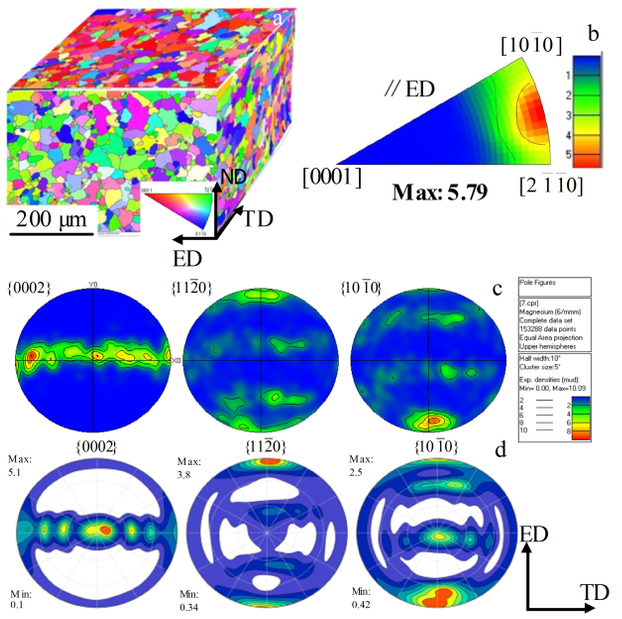

Fig. 4 Initial state of MgAZ31 extruded bar: (a) three-dimensional microstructure, (b) inverse pole figure, (c) micro-texture from EBSD, and (d) macro-texture from XRD

Table 1 Hardening parameters of each slip and twinning system in the simulation of Mg alloy under monotonic loading

Deformation mode	τ_0/MPa	T_1/MPa	θ_0/MPa	θ_1/MPa
Basal<*a*>	28	60	185	16
Prismatic<*a*>	85	10	200	250
Pyramidal<*c*+*a*>	110	15	120	400
Extension twin	45	0	150	400
Compression twin	210	100	345	400

show that at room temperature, the critical resolved shear stress (CRSS) of basal<*a*> slip[18] (approximately 0.45~0.81 MPa)< CRSS of the {10$\bar{1}$2} tension twin[19] (approximately 2~2.8 MPa)<CRSS of the prismatic<*a*> slip [20] (approximately 39.2 MPa)<CRSS of the pyramidal<*c*+*a*> slip [21] (approximately 45~81 MPa)<CRSS of the {10$\bar{1}$1} compression twin[19] (approximately 76~153 MPa) of magnesium and its alloys. Table 1 presents that the CRSS of the overall size order is consistent with the research value. Optimal hardening parameters play an important guiding role for future researchers to study the macro- and micro-deformation mechanisms of magnesium alloys.

The VPSC model was used to simulate and predict the true stress-strain curve of the AZ31 magnesium alloy under axial tension and compression. Experimental and simulated results are shown in Fig. 5. Notably, the AZ31 magnesium alloy exhibits serious axial tension-compression asymmetry. The axial tensile yield stress (144 MPa) is significantly higher than the axial compression stress (100 MPa), and the yield ratio is approximately 1.4. The strain hardening rate is asymmetrical. During axial compression, the strain hardening rate changes significantly, and the stress-strain curve is similar to an "S"

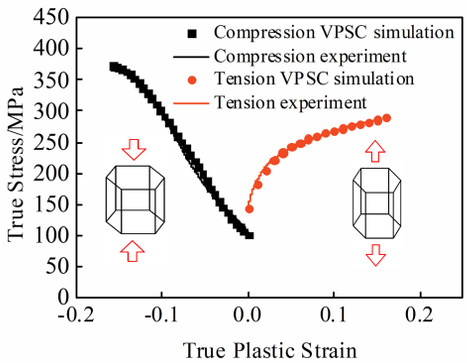

Fig.5 Correlation between experimental stress-strain and VPSC simulation results at room temperature

shape. During axial tension, the strain hardening rate has small change, and the stress-strain curve changes gradually. The stress-strain curves predicted by the VPSC model are in good agreement with the experimental results which can accurately reflect the stress-strain characteristics of each stage in the axial tension and compression plastic deformation process.

3 Results and Discussion

3.1 Analysis of deformation mechanism

Fig. 6 shows the prediction results of relative activity of deformation mechanism in the axial tension and compression deformation along the ED. Fig. 6a shows that during axial tension, the grain *c*-axis is subjected to compressive stress, the tensile twins are not easy to activate, and the relative activity is very small, which is less than 1%. Basal slip and prismatic slip play a dominant role in the entire deformation process. For extruded magnesium alloys, the {0002} basal plane of most grains tends to be parallel to the ED. At this time, the Schmid factor of the basal slip is low, which is in the hard orientation. Only when *F*/*A* reaches a high value, the base slip can be activated, resulting in a high yield strength of about 144 MPa during axial tensile process. With the increase in strain, the {0002} basal plane of most of the grains is basically parallel to the extrusion axis, and the basal slip is restrained. With the increase in stress value, the shear stress of non-basal slip reaches the CRSS. The dominant deformation mechanism changes from basal slip to prismatic<*a*> slip, the strain hardening rate is low, and the stress-strain curve is smooth, which is consistent with the results of Hutchinson[22]. When ε =0.02, the activity of the compression twin system increases slowly when the tensile twin is gradually depleted, because the slip is not enough to coordinate the compression strain of the *c*-axis, and the relative activity of the compression twin can coordinate the strain of the *c*-axis compression. Fig. 6b shows that during axial compression, the grain *c*-axis is subjected to tensile stress, which is conducive to the activating of tensile twins. When the tensile stress reaches 100 MPa, tensile twinning has a high activity due to its low CRSS. Therefore, at the early stage of deformation, the activity of the tensile twin system reaches 57%, leading to a lower yield stress, which is used as the main mechanism for coordinated deformation together with the basal slip. As the strain increases, the activity of pyramidal system increases gradually up to ~20%, which is consistent with a previous report[23]. When ε =0.04, the relative activity of the tensile twins is significantly reduced. At this time, the {0002} basal plane of a large number of grains has been rotated to a direction approximately perpendicular to the extrusion axis (Table 2). The tensile twinning of these grains is inhibited, while the CRSS of compression twinning at room temperature is high and it is difficult to activate; hence, the strain hardening rate increases rapidly, which is consistent with the results of Barnett[24]. At the same time, with the gradual increase in the strain, the activity of the basal, prismatic, and pyramidal slip system increases. Lou et al[25] believed that this phenomenon is closely related to the twin depletion, and the simulation results follow the same rule. When ε =0.12, the shear stress of the compression twin reaches the CRSS, the compression twin is activated, and the hardening rate decreases. These conditions occur because the accumulated stress during plastic deformation can be released due to a large degree of activation of the compression twin.

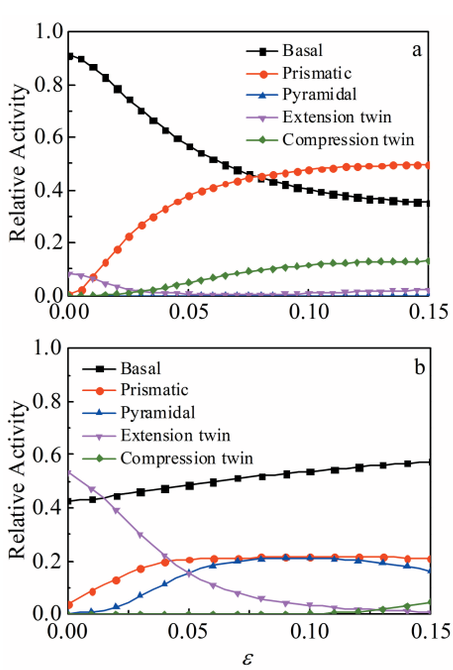

Fig.6 Predicted relative activity of deformation modes under uniaxial tension (a) and compression (b) along ED

3.2 Microstructural evolution

Fig. 7 shows the kernel average misorientation (KAM) and local misorientation distribution histogram of axial tension and compression at strain of 0.08 along the ED. The KAM map can be used to represent the local dislocation density and strain degree in the microstructure[26,27]. For a selected point, the average orientation difference between the point and all surrounding points (3×3) is taken as the local orientation difference of the point. The figure shows that the local

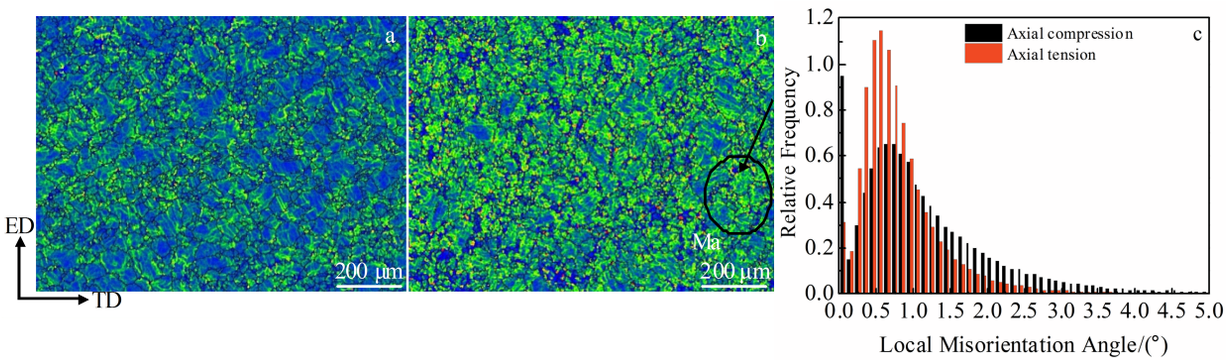

Fig.7 Local misorientation maps of axial tension (a) and compression (b) and local misorientation distribution histogram (c) along ED

orientation difference is concentrated at a low orientation difference angle (<1°) during axial tension, indicating that the dislocation density and strain are small. During axial compression, the local orientation difference is concentrated at the high orientation difference angle (>1°) and the distribution is relatively uniform, which is caused by the simultaneous opening of a variety of slip systems (basal, prismatic, and pyramidal slip) at the early stage of deformation, indicating that a large number of dislocations and large strains are produced during the axial compression process, with high dislocation density and strain.

Fig. 8 shows the EBSD and grain boundary structure maps of axial tension and compression at strain of 0.08 along the ED, in which the tension twin grain boundary is represented by a red solid line, and the compression twin grain boundary is represented by a blue solid line. Fig. 8a shows that during axial tension, an appropriate amount of $\{10\bar{1}2\}$ tensile twins and a small amount of $\{10\bar{1}1\}$ compressed twins can be observed, as shown by the black and white arrows, respectively. This phenomenon may be due to the non-uniformity of the initial texture and orientation (its *c*-axis is oriented to ED) of the grains in the initial extruded AZ31 magnesium alloy, which is clearly shown in the initial pole figure (Fig. 4c). Hence, during tension in the ED, the crystal might be subjected to the stress of adjacent grains, thereby causing the *c*-axis to stretch and generate tensile twins. Jain[28] obtained a similar observation. Fig. 8b shows that an appropriate amount of $\{10\bar{1}2\}$ tensile twins can be observed during axial compression in the ED, as shown by the black arrow in the figure. This contradicts the prediction in Fig. 6b that a large number of tensile twinning will activate in the initial deformation period.

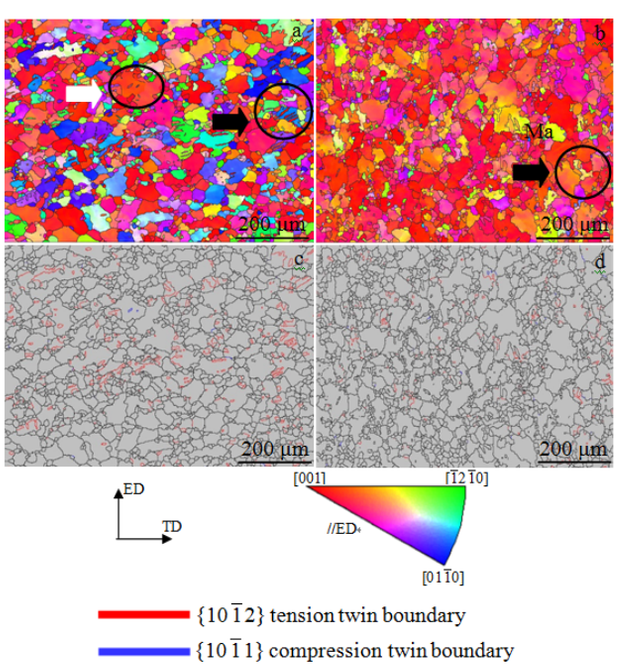

Fig.8 EBSD and boundary structure maps of axial tension (a, c) and compression (b, d) at the strain of 0.08 along ED

To explain this phenomenon, Fig.9 presents a typical EBSD maps and corresponding predicted tensile twin trace distribution of grain Ma. From the appearance, the twin Ta1 may nucleate at the upper grain boundary, which may be linked to the stress fluctuation at the upper grain boundary (the black arrow shown in Fig. 7b). This phenomenon is because the twinning nucleation at the grain boundary causes stress concentration. Adjacent grains may trigger twinning at the grain boundary to decrease stress concentration[29]. In addition, as can be seen from the color and twin trace of grain Ma, the grain Ma with high tension twin macro Schmid factor

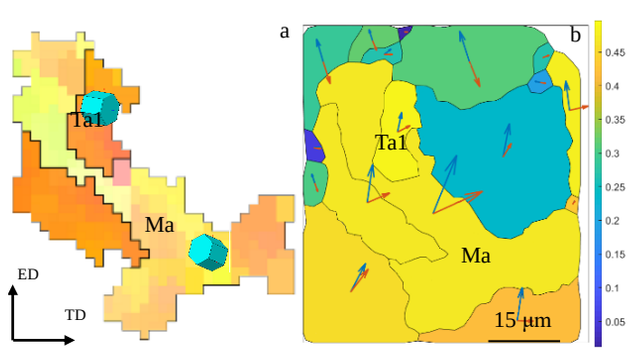

Fig.9 Typical EBSD map of grain Ma (a); predicted tension twin traces and tension twin macro Schmid factor distribution (b)

undergoes twin growth and fusion behavior[30], resulting in a surface phenomenon, where the $\{10\bar{1}2\}$ twin volume fraction decreases due to the disappearance of twin boundaries.

Fig. 10 shows the grain boundary map and grain boundary misorientation map of axial tension and compression of ε = 0.08 along the ED, in which the large-angle grain boundaries (>15°) are represented by black lines, and the small-angle grain boundaries (2° <θ<15°) are represented by green lines. Fig. 10a shows that during axial tension along the ED, two peaks appear in the range of <15° and 80°~90°, which represent small-angle grain boundaries and $\{10\bar{1}2\}$ tensile twins, respectively. Among them, the small-angle grain boundary peak is lower mainly due to the occurrence of twins, where the small-angle grain boundary absorption dislocation is transformed into a large-angle grain boundary. Fig. 10b shows that during axial compression along the ED, small-angle grain boundaries with higher peaks appear mainly due to the large number of activations of basal slip and pyramidal slip, and small-angle grain boundaries form at the grain and twin boundaries[31].

3.3 Texture evolution

Table 2 shows the pole figure simulation results along the ED at strain of 0.02, 0.04, 0.06, and 0.08, and the

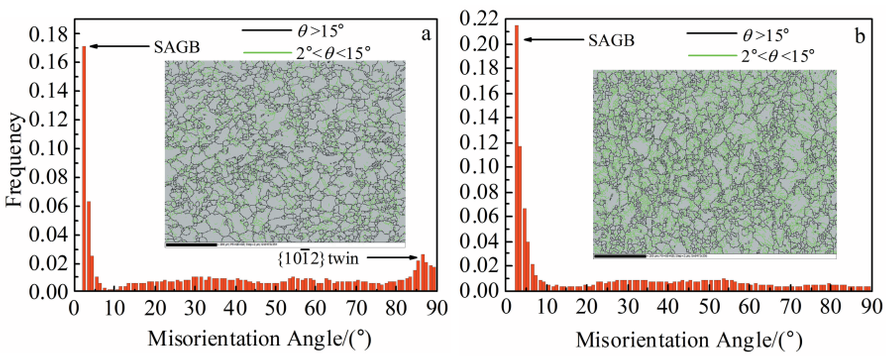

Fig.10 Grain boundary map and grain boundary misorientation map of axial tension (a) and compression (b) of ε=0.08 along the ED direction

Table 2 Predicted texture evolution under uniaxial tension and compression along ED to different strain levels

Strain	Tension	Compression
ε=0.02	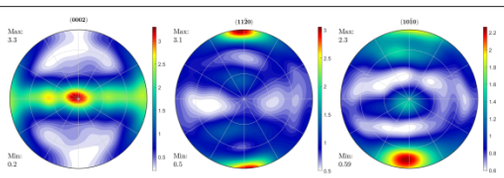	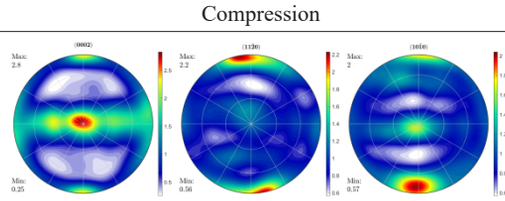
ε=0.04	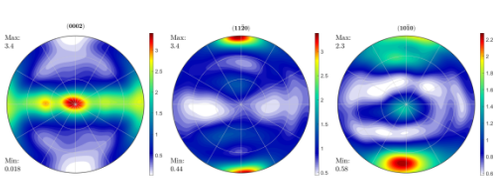	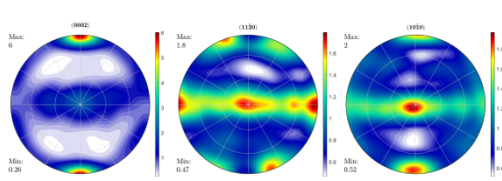
ε=0.06	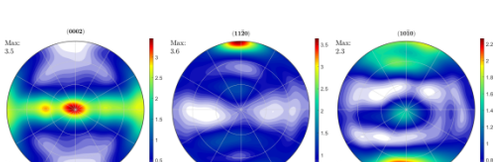	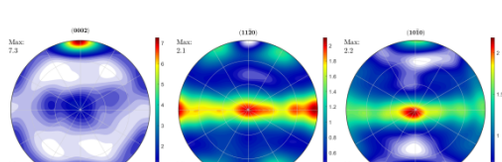
ε=0.08	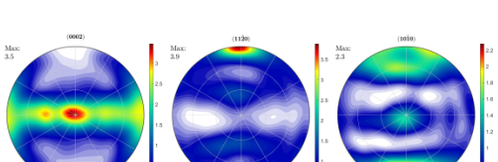	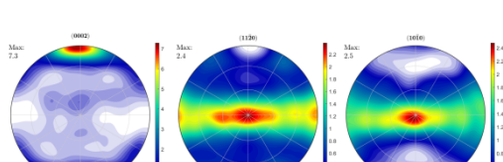
ε=0.08 (experimental)	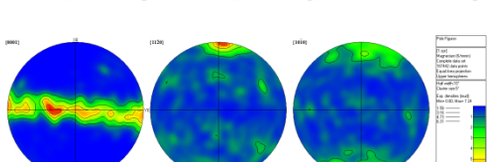	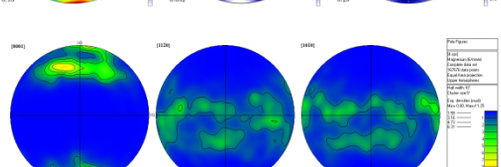

experimental results at strain of 0.08 with axial tension and compression. A comparison between simulation and experimental results show that the simulation results can reasonably reflect the texture evolution law in tension and compression along the ED. During axial tension along the ED, as the strain increases, regardless of the deformation amount, the {0002} and $\{11\bar{2}0\}$ pole figures change slightly, and only the texture strength increases. However, the pole density of $\{10\bar{1}0\}$ prismatic texture shifts to the ED due to the high activity of prismatic slip. During axial compression along the ED, the high activity of the tensile twins leads to the rotation of the grain *c*-axis to ~90°, which makes the pole density of the {0002} basal texture shift to the positive and negative direction of ED and also causes the pole density of the $\{11\bar{2}0\}$ and $\{10\bar{1}0\}$ prismatic texture to shift to the TD gradually.

4 Conclusions

1) The axial tension and compression experiment of extruded AZ31 magnesium alloy at room temperature can be simulated based on the modified VPSC model. The mechanism of tension-compression asymmetry and the law of texture evolution are analyzed from the perspective of micro-deformation mechanism. The twin growth and fusion behavior of the specimen in the later stage of deformation result in a surface phenomenon, and wherein the twin volume fraction decreases due to the disappearance of twin boundaries.

2) At the initial stage of axial tension, the basal slip is the dominant deformation mechanism. At this time, the orientation factor is low and orientation is in a hard orientation, resulting in high axial tensile yield stress. As the strain increases, the shear stress of non-basal slip reaches the CRSS, the dominant deformation mechanism becomes prismatic<*a*> slip, the strain hardening rate is lower, and the stress-strain curve is smooth. During the axial compression process, the tensile twins with a low CRSS value are highly activated during the initial deformation, leading to a lower yield stress. As the strain increases, the relative activity of the tensile twin decreases rapidly, and the hardening rate increases at the same time. When the strain reaches about 12%, the accumulated stress during plastic deformation can be released and the hardening rate decreases due to the massive activation of the compression twin.

3) The main reason for the difference in texture evolution between axial compression and tension is that the high activity of the tensile twins leads to the rotation of the grain orientation during the axial compression, while the high activity of prismatic slip during the axial tension makes the crystal grains move slowly.

References

1 Pan H, Qin G, Huang Y *et al*. *Acta Materialia*[J], 2018, 149: 350

2 Zeng Z, Stanford N, Davies C H J *et al*. *International Materials Reviews*[J], 2018(2): 1

3 Lu X, Zhao G Q, Zhou J X *et al*. *Vacuum*[J], 2018, 157: 180

4 Jia W, Ma L, Le Q *et al*. *Journal of Alloys and Compounds*[J], 2019, 783: 863

5 Jia W, Ning F, Ding Y *et al*. *Materials Science and Engineering* [J], 2018, 720(21): 11

6 Wang X, Shi T, Jiang Z *et al*. *Materials Science & Engineering* [J], 2019, 753(10): 122

7 He J, Mao Y, Gao Y *et al*. *Journal of Alloys & Compounds*[J], 2019, 786: 394

8 Niu Y, Song Z, Le Q *et al*. *Journal of Alloys and Compounds*[J], 2019, 801: 415

9 Gaskey B, Hendl L, Xiaogang W *et al*. *Acta Materialia*[J], 2020, 194: 558

10 Ren W J, Lin J B. *Materials Review*[J], 2015, 29(7): 89

11 Jia W T, Ma L F. *Journal of Materials Research and Technology* [J], 2020, 9(3): 4773

12 Lebensohn R A, Tomé C N. *Acta Metallurgica et Materialia*[J], 1993, 41(9): 2611

13 Zhang B, Li S, Wang H *et al*. *Materials*[J], 2019, 12(10): 1590

14 Chaudry, Hamad, Kim. *Crystals*[J], 2020, 10(2): 67

15 Zhao L Y, Chapuis A, Xin Y C *et al*. *Journal of Alloys & Compounds*[J], 2017, 710: 159

16 Agnew S R, Brown D W, TomécC N. *Acta Materialia*[J], 2006, 54(18): 4841

17 Kabirian F, Khan A S, Gnäupel-Herlod T. *International Journal of Plasticity*[J], 2015, 68: 1

18 Lou X Y, Li M, Boger R K *et al*. *International Journal of Plasticity*[J], 2007, 23(1): 44

19 Koike J. *Metallurgical and Materials Transactions A: Physical Metallurgy and Materials Science*[J], 2005, 36(7): 1689

20 Reed-Hill R E, Robertson W D. *Acta Metallurgica*[J], 1957, 5(12): 717

21 Agnew S R, Yoo M H, Tomé C N. *Acta Materialia*[J], 2001, 49(20): 4277

22 Hutchinson J W. *Proceedings of the Royal Society of London. Series A, Mathematical and Physical Sciences*[J], 1976, 348(1652): 101

23 Wang F, Agnew S R. *International Journal of Plasticity*[J], 2016, 81: 63

24 Barnett M R, Keshavarz Z, Beer A G *et al*. *Acta Materialia*[J], 2004, 52(17): 5093

25 Lou X Y, Li M, Boger R K *et al*. *International Journal of Plasticity*[J], 2006, 23(1): 44

26 Jin L, Dong J, Sun J *et al*. *International Journal of Plasticity*[J], 2015, 72: 218

27 Yang Y, Yang X, Xiao Z *et al*. *Materials Science and Engineering A*[J], 2017, 688: 280

28 Jain A, Duygulu O, Brown D W *et al*. *Materials Science & Engineering A, Structural Materials: Properties, Microstructure and Processing*[J], 2008, 486(1-2): 545

29 Niezgoda S R, Kanjarla A K, Beyerlein I J *et al*. *International Journal of Plasticity*[J], 2014, 56: 119

30 Wu W X, Jin L, Dong J *et al*. *Materials Science & Engineering A*

[J], 2014, 593: 48 [J], 2015, 650: 399

31 Jiang M G, Yan H, Chen R S. *Journal of Alloys and Compounds*

挤压态AZ31镁合金的拉压不对称性及微观组织

苏 辉[1]，楚志兵[1,2]，薛 春[1]，李玉贵[1]，马立峰[1]

(1. 太原科技大学 重型机械教育部工程研究中心，山西 太原 030024)

(2. 暨南大学 力学与建筑工程学院，广东 广州 510632)

摘 要：在考虑滑移和孪生两大塑性变形机制的基础上，通过修正的粘塑性自洽（VPSC）模型，模拟挤压态AZ31镁合金轴向拉-压过程中的力学行为及微观组织。结合EBSD实验与模拟，分析了不同变形机制对初始挤压态丝织构镁合金产生拉压不对称的机理以及塑性变形过程中的微观组织。结果表明，轴向拉伸变形初期以基面滑移系为主，由于基面滑移的施密特因子较低，导致屈服应力较高；随着应变的增加，棱柱面滑移成为主导变形机制，应变硬化率降低，应力-应变曲线较平稳；轴向压缩变形初期，临界剪切应力较低的拉伸孪晶大量开启导致屈服应力较低；随着拉伸孪晶相对活性的快速降低，应变硬化率迅速提高；轴向压缩后期，随着应力的持续升高，压缩孪晶开始启动，塑性变形积累的应力得到释放，导致应变硬化率降低。另外，从典型晶粒的颜色和孪晶迹线方面解释了沿ED方向压缩时孪晶体积分数较小的原因。

关键词：粘塑性自洽模型；拉-压不对称性；织构演化；塑性变形机制

作者简介：苏 辉，男，1994 生，硕士，太原科技大学材料学院，山西 太原 030024，E-mail：949500160@qq.com